A Numerical Prediction of the Turbulence Parameters in Two-Dimensional Ventilated Rooms

Ayad M. Salman*

Received on: 13 /10 /2010
Accepted on: 7 /4 /2011

Abstract

Turbulent flow in two-dimensional ventilated room has been numerically simulated in the present research. A modified form of Wilcox's two-equation LRN k-ω model is proposed for predicting internal turbulent ventilation flows. The modifications include adding a turbulent cross-diffusion term in the ω-equation, and re-establishing the closure constants and damping functions, with the application of the wall-function method. The turbulent cross-diffusion for specific rate, ω, is modeled with two parts: a second-order diffusion term and a first-order cross-diffusion term.

The air was used as the working fluid, and the length of ventilation enclosure (9 m), and height of ventilation enclosure (3 m). The study was made for Reynolds number values of ($Re=7.5\times10^3$).

A finite volume method is used with a staggered grid arrangement. The continuity, momentum and turbulence model equations are solved with hybrid method by using SIMPLE algorithm. A computer program in FORTRAN (90) was developed to carry on the numerical solution. The Computational algorithm is capable of calculating the hydrodynamic and turbulence properties such as the velocity, and turbulent kinetic energy, specific dissipation rate (ω), turbulent Reynolds stress, and terms of convection, production, diffusion, destruction, turbulent cross-diffusion and square root mean of fluctuating velocity. The results showed the peak value of velocity near the wall jet region and negative value of velocity near the bottom region (floor region) i.e. recirculating zone. The maximum value of turbulent kinetic energy near wall jet region in the first horizontal section of ventilation enclosure, and the profile become flattened in the second section of ventilation enclosure room. The same behavior in the turbulent Reynolds stress distribution because depending on velocity in his calculations. The same behavior between production term and destruction term but the values of production term is positive and the value of destruction term is negative. The distribution approximately symmetry.

The numerical results were compared with other previous theoretical results. The agreement was good, confirming the reliability of the proposed mathematical model and computational algorithm in investigating the performance of turbulence model in numerical simulation of turbulent ventilation flows.

Keywords: Turbulence Parameters, Ventilated Rooms, turbulent ventilation flows, LRN k-ω model, CFD.

* **Energy and Fuel Research Center, University of Technology/ Baghdad**

https://doi.org/10.30684/ etj.29.6.2
University of Technology-Iraq, Baghdad, Iraq/2412-0758

التنبؤ العددي لمتغيرات الاضطراب في غرف التهوية ثنائية البعد

الخلاصة

البحث الحالي يتضمن التمثيل العددي للجريان المضطرب في غرفة تهوية ثنائية البعد، تم استخدام نموذج الاضطراب ذو المعادلتين (k-ω) (نموذج Wilcox's) لرقم رينولدز الواطئ، حيث تم تطوير نموذج الاضطراب هذا ليتضمن إضافة حد عبر-الانتشار المضطرب في معادلة معدل التشتت النوعي (ω) واستخدام ثوابت تجريبية لنموذج الاضطراب لتلائم الجريان المضطرب لرقم رينولدز الواطئ، إضافة إلى استخدام دوال التخميد وتطبيق دالة الجدار في الحل، حد الانتشار-العرضي المضطرب في معادلة للمعدل النوعي للتشتت (ω) تم نمذجته بصيغة جزئيين: الأول حد الانتشار من الرتبة الثانية والحد الأخر من الرتبة الأولى.

استخدم الهواء كمائع عمل، طول حيز التهوية (9 m) وارتفاعه (3 m)، وأنجزت الدراسة لرقم رينولدز يساوي (7.5×10^3). استخدمت طريقة الحجوم المحددة مع الشبكة المنحرفة لحل معادلات حفظ الكتلة والزخم ومعادلتي نموذج الاضطراب تم باستخدام خوارزمية ألـ SIMPLE باستخدام الطريقة الهجينة، تم تطوير برنامج بلغة فورتران 9 لإنجاز الحل العددي. الخوارزمية الحسابية لها القدرة على حساب الخواص الهيدروديناميكية والاضطرابية مثل السرعة والطاقة الحركية المضطربة، المعدل النوعي للتشتت، إجهاد رينولدز، حد الحمل، حد الانتشار، حد التوليد، حد التدمير، وحد الانتشار-العرضي المضطرب والجذر التربيعي لمعدل تذبذب السرعة. بينت النتائج إن أعلى قيمة للسرعة بالقرب من منطقة النفث الجداري وقيم السرعة السالبة بالقرب من المنطقة السفلى لحيز التهوية أي منطقة إعادة التدوير (منطقة الدوامات)، أعلى قيمة للطاقة الحركية المضطربة بالقرب من النفث الجداري في المقطع الأفقي الأول من حيز التهوية، نفس السلوك لإجهاد رينولدز المضطرب بسبب اعتماده على السرعة في حسابه كما في أعلاه، نفس التصرف بين حد التوليد وحد التدمير ولكن قيم حد التوليد تكون موجبة وقيم حد التدمير سالبة ويكون التوزيع متناظر تقريبا.

لتأكيد النتائج العددية فقد تم مقارنتها مع النتائج النظرية السابقة وكان التوافق بين النتائج جيد مما يؤكد موثوقية النموذج الرياضي المقترح والخطوات العددية المتبعة في تخمين أداء نموذج الاضطراب في المحاكاة العددية لجريان الهواء في حيز التهوية.

Nomenclature

The following symbols are used generally throughout the text. Others are defined as and when used.

Symbols	Meaning
c_k, c_ω, $c_{\omega 2}$	Turbulence model constants
f_μ, f_k, f_ω	Damping functions of turbulence model
h	Height of inlet
H	Height of computational domain
I	Turbulence intensity
k	Turbulent kinetic energy
k^+	Dimensionless turbulent kinetic energy
L	Length of computational domain
p	pressure
Re	Reynolds number, $Re=U_{in}h/\nu$
R_t	Turbulent Reynolds number
t	Height of outlet
u	Velocity component in x-direction

u_*	Friction velocity
u', v'	Fluctuating velocities in x and y directions respectively.
$\overline{u'^2}$, $\overline{v'^2}$, $\overline{u'v'}$	Turbulent Reynolds stresses
u^+	Dimensionless velocity
u_{rms}	Root mean square of Reynolds stress $\sqrt{\overline{u'^2}}$
v	Velocity component in y-direction
x_j	Cartesian space coordinate
x, y	Cartesian coordinates
y^+	Dimensionless distance from wall surface

Greek Symbol

κ	Van karman constant
Γ	Exchange coefficient of dependent variable
μ	Molecular dynamic viscosity
μ_t	Turbulent dynamic viscosity
ν	Kinematics viscosity
ν_t	Turbulent kinematics viscosity
ρ	Density of air
σ_k, σ_ω	Turbulence Model constants
τ	Shear stress
τ_w	Wall shear stress
ω	Specific dissipation rate of k
ϕ	Dependent variable

Subscript Symbols

i,j	Tensor notation subscript
in	Inlet
p	First node near wall

1. Introduction

The air motion in a ventilated room is generally of an incompressible, non-isothermal and turbulent type. Nonetheless, indoor air flow possesses some specific features stemming from practical requirements on building ventilation. In many cases, ventilation flows are characterized by low-Reynolds-number (LRN) turbulence with mixing and recirculating air motion. Such general and specific flow characteristics must be well accounted for in turbulence modeling in order to make reliable system analyses by means of numerical simulations [1] .

CFD has been widely applied to various engineering flow problems. A field in which CFD is becoming increasingly active for system design, optimization and diagnosis is heating and ventilation in buildings. One of the basic objectives of ventilation is to Control and remove pollutants and/or excess heat to achieve the desirable

Indoor air quality and thermal environment. CFD has been proven to be an efficient approach for analyzing indoor air flow, heat transfer and contaminant dispersion processes. Particularly, it has often been employed to explore ventilation efficiency and effectiveness to indicate whether the air motion in a room is well organized. During the last few years there has been great interest in developing computational fluid dynamics (CFD) computer programs for predicting the air flow in ventilated rooms. The majority of these CFD programs are based on the solution of Navier—Stokes equations, the energy equation, the mass and concentration equations as well as the transport equations for turbulent velocity and its scale. The numerical solution of these equations in two and three dimensions has been applied to flow problems ranging from the ventilation enclosure to the prediction of smoke and fire spread in buildings [2].

This research is devoted to the application of CFD to predict the air movement in ventilated rooms. The fundamental flow and turbulence model equations are presented first and the methods used in solving them are then described. A brief review is given of the turbulence models that can be used to describe the effect of turbulent eddies in the flow. The application of CFD models to solve a range of ventilation problem is also given. The turbulence model is specially an important aspect of CFD. It is obvious that room air flow will be turbulent because of geometry and practical velocity levels, but it will not always be a fully developed turbulent flow. Some of the widely used models are discussed such as the k- ω model.

2. Objectives of the Present Work

The primary objective of this project is to evaluate the usefulness of computational fluid dynamic techniques in modeling room air flow. This evaluation process involves the implementation of turbulent modeling to air flow, by examining the effect of turbulence parameters on the accuracy of the predicted results. This will be achieved by numerical simulation to continuity, momentum, and turbulent equations for steady incompressible flow in ventilation room. Pressure based finite volume method with staggered grid is used in numerical solution. Cartesian velocity components and pressure are used as a dependent variable.

3. Mathematical Model

The partial differential equations are the best way to represent the physics of any engineering problems, like the turbulent flow problems. In this section can be used to predict the turbulent flow in two-dimensional ventilation room. Figure (1) shows the configuration and dimensions of the investigated flow field, for steady state, incompressible, two-dimensional Turbulent flow. Where the dimensions are: L=9.0 m, H=3.0 m, h =0.168 m, t=0.48 m.

3.1 Governing equations

The governing equations of motion based on Navier-Stokes equations conservation form for continuity, momentum and transport equations of turbulence (k-ω turbulence model equations) are as follows [2], [3]:

For continuity equation

$$\frac{\partial(\rho u_j)}{\partial x_j} = 0 \qquad (1)$$

For momentum equation

$$\frac{\partial(\rho u_i u_j)}{\partial x_j} = -\frac{\partial p}{\partial x_i} + \frac{\partial}{\partial x_j}\left[\mu\left(\frac{\partial u_i}{\partial x_j} + \frac{\partial u_j}{\partial x_i}\right)\right] - \frac{\partial}{\partial x_j}\left(\rho\overline{u_i' u_j'}\right) \quad (2)$$

Where the term $(-\rho\overline{u_i' u_j'})$ is the viscous stress tensor (turbulent Reynolds stress)

$$-\rho\overline{u_i' u_j'} = \mu_t\left(\frac{\partial u_i}{\partial x_j} + \frac{\partial u_j}{\partial x_i}\right) - \frac{2}{3}\rho k\delta_{ij} \quad (3)$$

$\delta_{ij}=1$ for i=j and $\delta_{ij}=0$ for i≠j, in Cartesian coordinates system expressed as

$$\left.\begin{aligned} -\rho\overline{u'^2} &= 2\mu_t\frac{\partial u}{\partial x} - \frac{2}{3}\rho k \\ -\rho\overline{v'^2} &= 2\mu_t\left(\frac{\partial v}{\partial y}\right) - \frac{2}{3}\rho k \\ -\rho\overline{u'v'} &= -\rho\overline{v'u'} = \mu_t\left(\frac{\partial u}{\partial y} + \frac{\partial v}{\partial x}\right) \end{aligned}\right\} \quad (4)$$

3.2Turbulence Transport Equations

The k-ω model is gaining in popularity, the model was proposed by Wilcox [3]. In this model the standard k equation is solved, but as a length determining equation ω is used. This quantity is often called specific dissipation from its definition $\omega \propto \varepsilon/k$. In the k-ω model, it is assumed that the turbulence is characterized by a velocity scale, $k^{1/2}$, and a length scale, $k^{1/2}/\omega$. The eddy viscosity is thus formulated as $\nu_t \sim k/\omega$. Wilcox termed ω as the specific dissipation rate of k, which is actually the reciprocal turbulent time scale, $1/\tau$. The transport equations for k and ω, together with the equations for continuity and momentum, form the mathematical description. In Wilcox's k-ω model the model transport equations for k and ω in are as follow:

$$\frac{\partial(\rho u_j k)}{\partial x_j} = P_k - c_k\rho\omega k + \frac{\partial}{\partial x_j}\left[\left(\mu + \frac{\mu_t}{\sigma_k}\right)\frac{\partial k}{\partial x_j}\right] \quad (5)$$

Where P_k is the production of turbulence energy, and for incompressible flow takes the form

$$P_k = -\rho\overline{u_i' u_j'}\frac{\partial u_i}{\partial x_j} = \mu_t\left(\frac{\partial u_i}{\partial x_j} + \frac{\partial u_j}{\partial x_i}\right)\frac{\partial u_i}{\partial x_j} \quad (6)$$

$$\frac{\partial(\rho u_j \omega)}{\partial x_j} = c_{\omega 1}\frac{\omega}{k}P_k - c_{\omega 2}\rho\omega^2 + \frac{\partial}{\partial x_j}\left[\left(\mu + \frac{\mu_t}{\sigma_\omega}\right)\frac{\partial \omega}{\partial x_j}\right] \quad (7)$$

With the Kolmogorov-Prandtl relation, the eddy viscosity, μ_t, is obtained from

$$\mu_t = c_\mu\frac{\rho k}{\omega}$$

The values of model constants are tabulated in table (1).

3.3 The Low Reynolds Number (LRN) k-ω Model

A model which is being used more and more is the Wilcox's k-ω model (standard k-ω model). The standard k-ω model can actually be used all the way to the wall without any modifications. The Low Reynolds Number (LRN) k-ω Model read as the same equations above but the changes on the standard model are [4], [5].

The cross diffusion terms will be add to the ω equation as

$$cross\,diffusion\,term = c_\omega \frac{\mu_t}{k}\left(\frac{\partial k}{\partial x_i}\frac{\partial k}{\partial x_j}\right) \quad (9)$$

The turbulence constants for Low Reynolds Number turbulence model becomes as

$$c_\mu = c_\mu f_\mu \,,\ c_k = c_k f_\mu \,,\ c_\omega = c_w f_\mu \quad (10)$$

The damping function for high Reynolds $f_\mu=1$, The damping functions for low Reynolds number for the eddy (turbulent) viscosity by the turbulence models are listed below:

$$f_\mu = 0.025 + \left\{1 - \exp\left[-\left(\frac{R_t}{10}\right)^{3/4}\right]\right\} \times \left\{0.975 + \frac{0.001}{R_t}\exp\left[-\left(\frac{R_t}{200}\right)^2\right]\right\} \quad (11)$$

$$f_k = 1 - 0.722\exp\left[-\left(\frac{R_t}{10}\right)^4\right] \quad (12)$$

$$f_\omega = 1 + 4.3\exp\left[-\left(\frac{R_t}{1.5}\right)^{1/2}\right] \quad (13)$$

Where R_t is the turbulent Reynolds number, and

$$R_t = k/(\omega\nu) \quad (14)$$

$$\text{Or } R_t = \nu_t/\nu \quad (15)$$

In low Reynolds number (LRN) k-ω turbulence model, the closure constants are revised in table (2) [4], [5].

If z represents k or ω, the turbulence transport equations in a two equations model, in general form for the turbulent kinetic energy k, and the dissipation rate of turbulent kinetic energy ω, these equations can be written as [6].

$$\frac{\partial(\rho u_j z)}{\partial x_j} = P_z + \frac{\partial}{\partial x_j}\left[\left(\mu + \frac{\mu_t}{\sigma_k}\right)\frac{\partial z}{\partial x_j}\right] - E_z + CD_z \quad (16)$$

Where P_z is the production term, E_z is the destruction term and CD_z is cross-diffusion term. The two additional terms in ω-equation as compared with Wilcox's model. These terms are given in table (3).

3.4 Boundary Conditions

Several different boundaries were encountered in this work, inflow, outflow, solid wall and homogeneous boundaries. Each has its own specification, which are summarized below.

3.4.1 Inlet Flow

These have been used in the computation of ventilation flows with two equation turbulence models. The velocities and transport quantities over the inlet boundary are usually prescribed, either from experimental data from pre-calculated distribution for, e.g., channel flow [2], [7].

$$\left.\begin{aligned} u &= U_{in} \\ v &= 0 \\ k_{in} &= \frac{3}{2}(IU_{in})^2 \\ \omega_{in} &= C_\omega \frac{k_{in}^{1/2}}{\ell_{in}} \end{aligned}\right\} \quad (17)$$

Where I is the turbulence intensity and can take a value between 0.01 to 0.1 (it is usally set been in a range of (0.02 ~ 0.04) for reciculating flows), see [8], C_ω is a constant (C_ω=1/0.09) and ℓ_{in} is specified as fraction of inlet size $(\ell_{in} = h/10)$.

3.4.2 Outlet Flow

Neumann conditions have often been set for the flow variables at outlet flow boundaries, giving as

$$\frac{\partial u}{\partial x}=\frac{\partial v}{\partial x}=\frac{\partial k}{\partial x}=\frac{\partial \omega}{\partial x}=0 \qquad (18)$$

3.4.3 Wall Boundary Condition

The common kinematic (non-porous wall) and viscous (no slip) conditions were used at the walls. The wall boundary conditions can be summarized as [5].

$$\left.\begin{array}{l} u=v=k=0 \\ \dfrac{\partial \omega}{\partial x}=\dfrac{\partial \omega}{\partial y}=0 \end{array}\right\} \qquad (19)$$

The natural way to treat wall boundaries is to make the grid sufficiently fine so that the sharp gradients prevailing there are resolved. Often, when computing complex flow, that requires too much computer resources. An alternative is to assume that the flow near the wall behaves like a fully developed turbulent boundary layer and prescribe boundary conditions employing wall functions. The assumption that the flow near the wall has the characteristics of that in a boundary layer if often not true at all. However, given a maximum number of nodes that can afford to use in a computation, it is often preferable to use wall functions which allows us to use fine grid in other regions where the gradients of the flow variables are large. When wall functions used k and ω are prescribed as [9], [10].

$$k_p=(c_k)^{-0.5}u_p^2 \qquad (20)$$

$$\omega_p=\frac{6\nu}{c_{\omega 2}y_p^2} \qquad (21)$$

3.5 Turbulent Quantities

For the components parallel to the wall we prescribe the friction velocity, wall shear stress, and dimensionless quantities as [11], [7].

$$u_*=\frac{\kappa u_p}{\ln(Ey^+)} \qquad (22)$$

$$\tau_w=\mu_{t,p}\frac{u_p}{y_p}=\rho u_*^2 \qquad (23)$$

$$y^+=\frac{\rho u_* y_p}{\mu} \qquad (24)$$

$$u^+=\frac{u}{u_*} \qquad (25)$$

$$k^+=\frac{k}{u_*^2} \qquad (26)$$

Where κ is Von Karman constant and its value 0.4187, the value of the E constant is 8.8 [12]. Generally the law of the wall is valid for $30 < y^+ < 60$.

4. Numerical Analysis

The mathematical formulation of the fluid flow problem is governed by basic conservation of mass, momentum and turbulence model equations.

4.1 Descretization Equation for Two Dimensions

A portion of a two-dimensional grid is shown in Fig. (2). For the grid point (P), points (E) and (W) are its x-direction neighbors; (N) and (S) are the y-direction neighbors, locations of them exactly midway between the neighboring points [13], [14].

The descretization equation based on the differential equations of the momentum equations and turbulence model equations can easily be seen to be:

$$a_P\phi_P = a_E\phi_E + a_W\phi_W + a_S\phi_S + a_N\phi_N + S_P \quad (27)$$

And

$$a_P = a_E + a_W + a_S + a_N + S_P \quad (28)$$

At this point, it is interesting to examine the physical significance of viscous coefficients in the descretization equations. The neighbor coefficients ($a_E,\ldots,a_N$) represent the connective between the point (P) and the corresponding neighbor. The center point coefficient (a_P) is the sum of all neighbor coefficients. But the source term (S_P) in the momentum equations and turbulence model equations.

4.1.1 Dimensional Descretization

The general form of the transport equation may be written as [13]:

$$\frac{\partial}{\partial x_i}(J_i) = S_\phi \quad (29)$$

Where

$$J_i = \rho u_i \phi - \Gamma_\phi \frac{\partial \phi}{\partial x_i} \quad (30)$$

Where J_i represents all the flux due to both diffusion and convection. The source term may be expressed as a linear expression:

$$S_\phi = b\phi_P + c \quad (31)$$

The source term in above equation can be summarizing in table (4).

4.2 Solution of the Descretized Equation (Pressure-linked Descretization Method)

One of the most widely used method that links the velocity field to the pressure field; in order to satisfy the continuity is the (SIMPLE) presented by [13] [Semi Implicates Methods for Pressure Linked Equation], in the solution presented below a staggered grid is employed. The SIMPLE assumes that,

$$\left.\begin{aligned} P = P^* + P' \;;\quad u = u^* + u';\\ v = v^* + v' \end{aligned}\right\} \quad (32)$$

For the computational convenience, $\sum_i a_i u_i'$, $\sum_i a_i v_i'$ are set to zero, we get

$$\left.\begin{aligned} u_e = u_e^* + \frac{(P_P' - P_E')\Delta y}{a_e} \;;\\ v_n = v_n^* + \frac{(P_P' - P_N')\Delta x}{a_n} \end{aligned}\right\} \quad (33)$$

Substituting these velocities into the continuity equation we obtain,

$$\sum_i a_i P_p' = \sum_i a_i P_i + c \quad (34)$$

Where c must equal to zero to get more accuracy.

$$\sum_i a_i = a_E + a_W + a_N + a_S \quad (35)$$

$$\sum_i a_i P_P' = a_E P_E' + a_W P_W' + a_N P_N' + a_S P_S' \quad (36)$$

The procedure for applying the SIMPLE method can be summarized as:

The procedure for applying the SIMPLE method can be summarized as:

1. Use any suitable initial values.
2. Guess the pressure field p'.

3. Solve the momentum equations to find out u^* and v^*, equation (32).
4. Solve the p' equation, equation (34).
5. The pressure field is obtained by adding p' to p^* .
6. Obtain the velocity components u and v from equation (33).
7. Any variable that influences the solution is solved for (k and ω) equations.
8. Iterate using the correct pressure p as the new guessed pressure p^*, return to step (3) and
repeat the whole procedure until converged solution is obtained.

Since the solution is non-linear, it is sometimes necessary to under relax the solution to avoid divergence. Under-relaxation is implemented as,

$$\phi_P^{\,r} = \alpha\,\phi_P + (1-\alpha)\,\phi_P^{\,\circ} \qquad (37)$$

Where

$\phi_P^{\,r}$ is the new under-relaxed value of ϕ_P.

$\phi_P^{\,\circ}$ is the value of ϕ_P from the previous iteration.

ϕ_P is the obtaining value.

The value of the under-relaxation factor (α) should be in the range ($0 < \alpha \leq 1$). Typical values for ($\alpha = 0.5$) for [u, v, k and ω] and ($\alpha = 1$) for (P). A computer program in (Fortran 90) was developed to execute the numerical algorithm which is mentioned above.

5. Results and Discussion

The present calculations was carried out for the flow at $Re=7.5\times10^3$ ($Re=(U_{in}h/\nu)$, $U_{in}=0.71$ m/sec,) as Low Reynolds Number for turbulent ventilated flow and L/H=3 in a two-dimensional turbulent flow of confined enclosure ventilation room. A Finite volume code is used, the calculations were performed with (70×58) cells for x and y direction respectively. For space discretization, hybrid scheme is used.

Figure (3) shows velocity vector plots of computational domain of ventilation enclosure. This accounts for the entrainment process between the wall jet and it's surrounding. A wall jet initiated from inlet reaches the opposite wall and overall recirculation (vortex) is created.

Figure (4) shows the distribution prediction of velocity profiles at vertical cross section x=H and x=2H. We see positive values of velocity near wall jet region as peak velocity in the wall jet region. Then decrease toward the region of recirculation (re-attachment region) i.e. near the floor. This is also reflected in figure (5) in the distributions along the two horizontal section bottom (y=h/2) and top (y=H-h/2).

Figures (6) and (7) show the distribution of turbulent kinetic energy in vertical section at x=H and x=2H, notice that the maximum value of the kinetic energy in region near the wall jet and decreases in the region near the floor also we see the profile more flattened in x=2H . Figure (7) illustrates the distribution of turbulent kinetic energy in top (y=H-h/2) and bottom (y=h/2), we show the value of turbulent kinetic energy in top region is grater than in bottom region because the value of velocities in these region.

Figure (8) shows the distribution of Reynolds stress in the section of the vertical at x = H and x = 2H, where we note that the largest value

of Reynolds stress at a section blowing wall jet of any slot-equipped because of the velocity have the greatest value in this region and gradually decreases in other areas that up to its lowest value in the region close to the floor region. A figure (9) shows the distribution of Reynolds stress in the horizontal section at the bottom y=h/2 and the top y=H-h/2 where we note clear oscillation in the values of Reynolds stress in the bottom region than it is in the top region.

Figures (10) shows the distribution of specific dissipation rate, ω, the profile of ω in the vertical cross section at x=H and x=2H the results are similar in behavior, the variation can be mainly observed from the horizontal distribution as shown in figure (11), where the peak value of the specific dissipation rate in section y=H-h/2 as sharper peak a riser. The largest contribution, usually, occurs in the immediate proximity of the wall, where the gradients for both k and ω are rather large. This peak corresponds to the turning separation point in front of the opposite wall, where the wall-jet flow starts to descend.

Figure (12) shows the vertical distribution of the production and destruction, terms at x=2H, where we note that the values of production term are positive and which represents the gain while the values of destruction loss. We observe the same behavior in the values of the positive end of production and the losses represented by the dispersion term, but the behavior is different as shown in figure (13). The production term, as expected, has been reduced. Along the central line of the wall jet region (y = H □□h/2), there is a peak in the balance (budgets) in front of the opposite wall. This peak is largely damped in the ω-equation, owing to the turbulent cross-diffusion term.

Figure (14) shows the distribution of the convection and diffusion terms in a vertical section at x = 2H, where the behavior a close between them, while we note the different (disposal) of the various through section of the horizontal at y=H-h/2 and the values are close in the middle of the field arithmetic, while there is variation in the values in the areas of the beginning and the end of the horizontal section and as shown in figure (15).

Figure (16) shows the distribution of turbulent cross diffusion through the vertical section at x=2H, where we note that a value ranging between 0 and -8 and close to zero in the middle of the vertical section. As shown in figure (17) the distribution of the turbulent cross diffusion through the horizontal section at y=H-h/2 where we note there oscillating (fluttering) in values, especially in the region near the blowing wall jet while takes the stability form in the region far from the slot processing. The turbulent cross-diffusion term plays a role mainly in the near wall region, where the gradients of *k* and □□are rather large and usually of opposite signs. This will therefore drag down the specific dissipation rate and increase the kinetic energy.

Figure (18) shows horizontal distribution for u_{rms} (root mean square of fluctuating velocity) where we note the different behavior in the area near the exhaust wall jet, but here the disposal or different behavior in the vicinity of the ground floor region also built figure (19) vertical distribution at the center line of section x=2H.

Figures (20) and (21) show comparison between velocity profile at x/H=2 and y=H-h/2 respectively with the experimental results of [15]. The best agreement at bottom region and the difference reach to (12.7%) approximately at y/H=0.93 in figure (20), while in figure (21) the best agreement in wall jet region and the maximum difference between these results reach to (15.8%) approximately at (x/H=2.7). Figure (22) shows the comparison between distribution of velocity profile at center line of vertical section with experimental data [16], this shows good agreement. Figure (23) show the distribution of dimensionless streamwise velocity in comparison with data predicted from models by [8] for channel flow and $Re=10^4$, with aspect ratio (AR=5). Where the program was executed to these conditions, the present model yield very good agreement with this result.

6. Conclusions

A modified form of Wilcox's two-equation LRN k-ω model is used for predicting internal turbulent flows in ventilation rooms. The modifications include adding a turbulent cross-diffusion term in the ω-equation, and re-establishing the closure constants and damping functions. The model combines a wall function and low-Reynolds-number (LRN) approach. The modified model reproduces correct near wall asymptotic behaviors, and leads to prediction of turbulent flow in ventilated rooms.

The peak value of velocity near the wall jet region and negative value of velocity near the bottom region (floor region) i.e. recirculating zone.

The maximum value of turbulent kinetic energy near wall jet region in the first horizontal section of ventilation enclosure, and the profile become flattened in the second section of ventilation enclosure room. The same behavior is seen for turbulent Reynolds number.

A similar behavior between production term and destruction term was seen. The distribution is approximately symmetry.

The distribution of turbulent cross diffusion term is symmetry approximately and the value lies between 0 and -8. A turbulent cross-diffusion term was added to the w-equation in analogy to its molecular counterpart.

Turbulent cross-diffusion term in modified ω-equation play a role in the near wall region where the gradients of k and ω are rather larger. This will drag down the specific dissipation rate and increase the turbulent kinetic energy.

The peak in the horizontal ω-distribution at section y=H-h/2 is the greatest and its due larger to the turning or separation point in front of opposite wall where the wall-jet flow starts to descend.

The present model has shown a reasonable ability to simulate the turbulent flows in two-dimensional ventilated rooms.

References

[1] Davidson, L., Nielsen, P. V. and Topp, C., 2000, "Low-Reynolds Number Effects in Ventilation Rooms: A Numerical Study". Elsevier Science Ltd. Air Distribution in Rooms, (ROOMVENT), PP. 307-312.

[2] Awbi, H. B., 1991, "Ventilation Buildings", E & FN SPON INC.

[3] Wilcox, D. C. 1994 "Turbulence modeling for CFD" DCW Industries, Inc., La Canada, California.

[4] Bredberg, J. , Peng S.-H. and Davidson, L., 2002, "An Improved k-ω turbulence model Applied to

Rcirculating Flow" Int. J. Heat and Fluid Flow, Vol. 23, pp. (731-743).

[5] Sunde´n, B., Jia, R. and Abdon, A., 2004, "Computation of combined turbulent convective and impingement heat transfer", Int. J. Numerical Methods for Heat & Fluid Flow, Vol. 14, No. 1, pp.(116-133).

[6] Peng, S.-H., Davidson, L., Holmberg, S., 1996, "Performance of Two-Equation Models for Numerical Simulation of Ventilation Flow", 15th Int. Conf. on Air Distributions in Rooms, Yokohama, Japan, Vol. 2, pp. 153-160.

[7] CFD-FASTRAN , Theory Manual , Version 2003, CFDRC Confidential, SINTEF applied mathematics, Oslo, Norway, www.cfdrc.com.

[8] Abe, k., Kondoh, T., Nagano, Y., 1994, "A New Turbulence Model for Predicting Fluid Flow and Heat Transfer in Separating and Reattaching Flows –I. Flow field Calculation", Int. J. Heat and Mass Transfer, Vol. 37, pp. 139-151.

[9] Wang and S. Komori, (1998), "Prediction of duct Flows with Pressure-Based Procedure," J. Numerical Heat Transfer, Part A, Vol. 33, PP. 723-784.

[10] Bredberg, J., Peng S.-H., Davidson, L., 2000, "On The Wall Boundary Condition for Computing Turbulent Heat Transfer with k-ω Models", Proceedings of the ASME Heat Transfer Division , Nov 5-10, 2000, Orlando, Florida, USA.

[11] Bredberg, J., 2001, "On Two-equation Eddy-Viscosity Models" Internal Report 01/8, Department of Thermo and Fluid Dynamics Chalmers University of Technology, Göteborg, Sweden.

[12] Launder, B. E., and Spalding, B. D., (1974), "The Numerical Computation of Turbulent Flow," J. Compt. Meth. Appl. Mech. Enging., Vol. 3, PP. 269-289.

[13] Patankar, S., 1980, "Numerical Heat Transfer and Fluid Flow" McGraw-Hill, New York.

[14] Versteegh ,H. K. and Malalasekera W., 1995, "An Introduction to Computational Fluid Dynamics: Finite Volume Method" Harlow, England: Longman Scientific & Technical. [15] Davidson, L., Nielsen, P. V., 1996, "Large Eddy Simulation of the Folw in a Three-dimensional Ventilated Room", 15th Int. Conf. on Air Distribution in Rooms, Yokohama Japan, Vol. 2, pp. (161-168).

[16] Muller, D., Davidson, L., 2000, "Comparison of Different Subgrid Turbulence Models and Boundary Conditions for Large-Eddy Simulations of Room Air Flows", 7th International Conference on Air Distribution in Rooms, Room vent, pp. 301-306.

Table (1) Turbulence model constants for the k-ω equations.

Constant	c_μ	c_k	$c_{\omega1}$	$c_{\omega2}$	σ_k	σ_ω
Value	1.0	0.09	0.56	0.075	2.0	2.0

Table (2) Turbulence model constants for low Reynolds number k-ω model.

Constant	c_μ	c_k	c_ω	$c_{\omega1}$	$c_{\omega2}$	σ_k	σ_ω
Value	1.0	0.09	0.75	0.42	0.075	0.8	1.35

Table (3) Production, destruction and cross diffusion terms in k-ω model.

Term	P_z	E_z	CD_z
k-equation	$\mu_t\left(\frac{\partial u_i}{\partial x_j}+\frac{\partial u_j}{\partial x_i}\right)\frac{\partial u_i}{\partial x_j}$	$c_k f_k \rho\omega k$	0
ω-equation	$c_{\omega1} f_\omega \frac{\omega}{k}\left[\mu_t\left(\frac{\partial u_i}{\partial x_j}+\frac{\partial u_j}{\partial x_i}\right)\frac{\partial u_i}{\partial x_j}\right]$	$c_{w2}\rho\omega^2$	$c_\omega \frac{\mu_t}{k}\left(\frac{\partial k}{\partial x_j}\frac{\partial \omega}{\partial x_j}\right)$

Table (4): Source term in the governing (PDE's).

Equation	ϕ	Γ	S
Continuity	1	0.0	0
Momentum	u	μ_e	$-\frac{\partial p}{\partial x}+\frac{\partial}{\partial x}\left(\nu_e\frac{\partial u}{\partial x}\right)+\frac{\partial}{\partial y}\left(\nu_e\frac{\partial v}{\partial x}\right)$
	v	μ_e	$-\frac{\partial p}{\partial y}+\frac{\partial}{\partial x}\left(\nu_e\frac{\partial u}{\partial y}\right)+\frac{\partial}{\partial y}\left(\nu_e\frac{\partial v}{\partial y}\right)$
Turbulent Kinetic energy	k	$\mu+\frac{\mu_t}{\sigma_k}$	$P_k - C_k f_k \omega k$
Specific dissipation	ω	$\mu+\frac{\mu_t}{\sigma_\omega}$	$\frac{\omega}{k}(C_{\omega1} f_\omega P_k - C_{\omega2}\rho\omega k)+C_\omega\frac{\mu_t}{k}\left(\frac{\partial k}{\partial x}\frac{\partial \omega}{\partial x}+\frac{\partial k}{\partial y}\frac{\partial \omega}{\partial y}\right)$

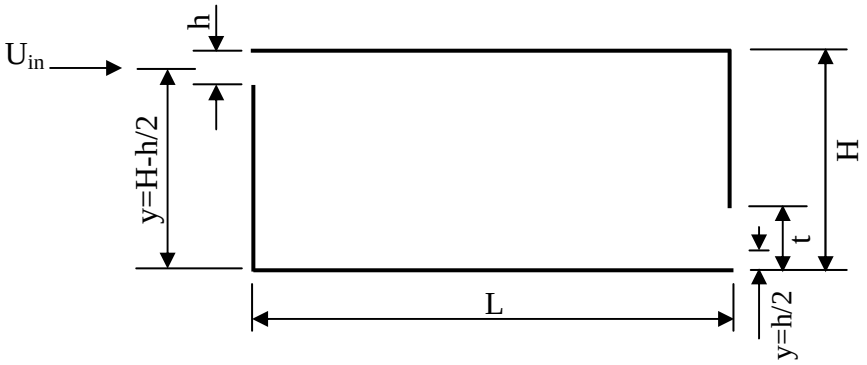

Figure (1): Show configuration of the investigated ventilated room.

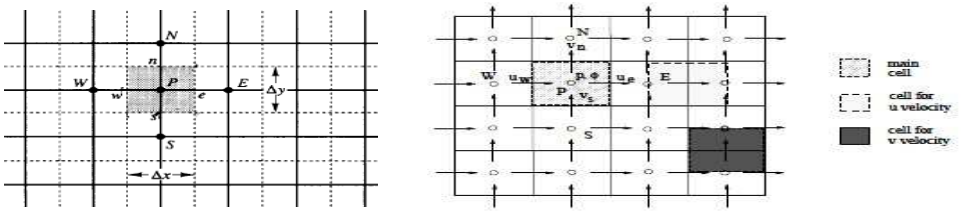

a) Two dimension grid. b) Staggered grid.

Figure (2): Show control volume for two-dimensional

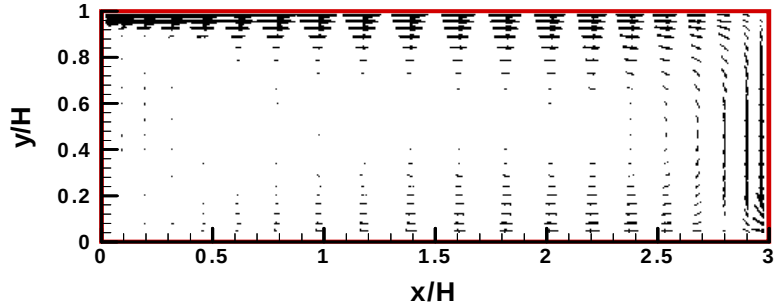

Figure (3): Velocity vector in ventilation room.

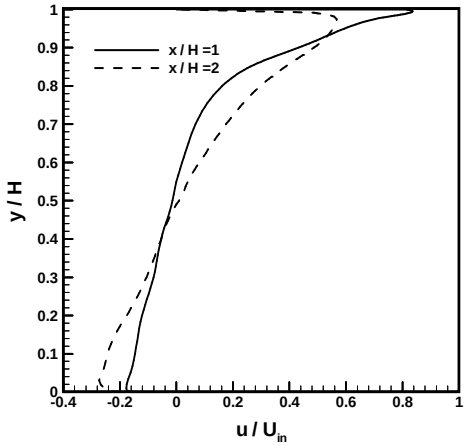

Figure (4) Distribution of axial velocity profile at vertical cross section for

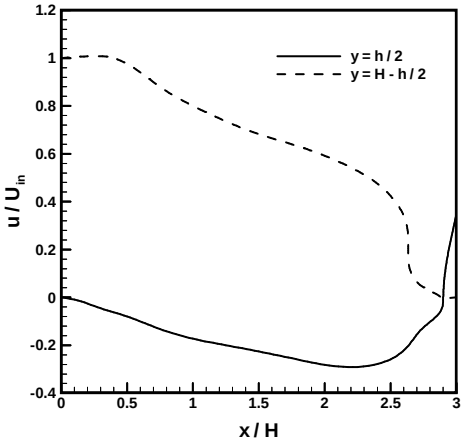

Figure (5) Distribution of axial velocity profile at horizontal cross section for different location of y.

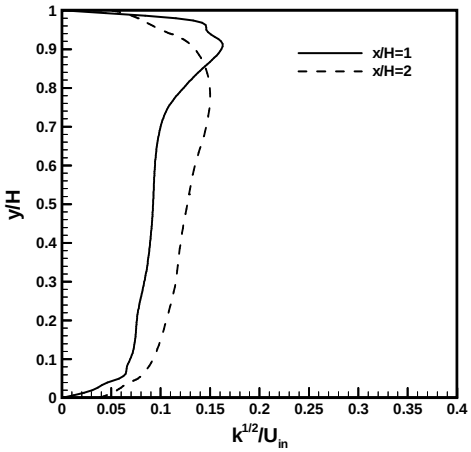

Figure (6)Distribution of turbulent Kinetic energy profile at vertical cross section for different location of x.

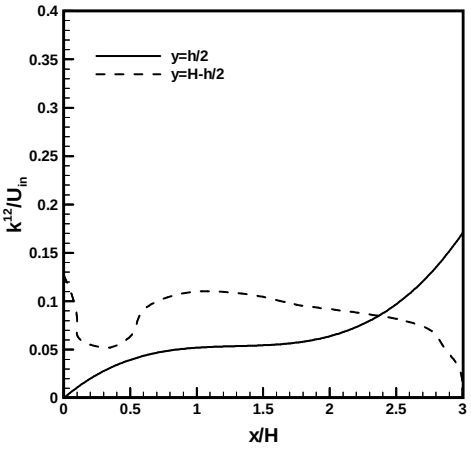

Figure (7) Distribution of turbulent kinetic energy profile at horizontal cross Section for different location of y.

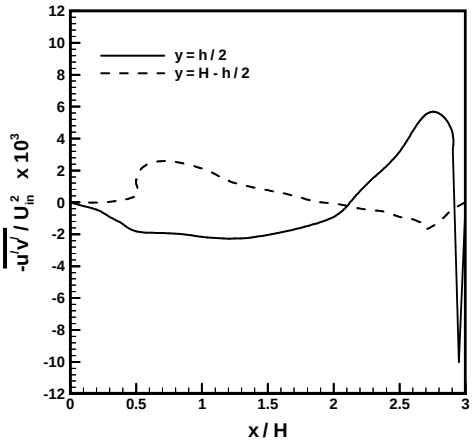

Figure. (8): Distribution of Reynolds stressat vertical cross section for different location of x.

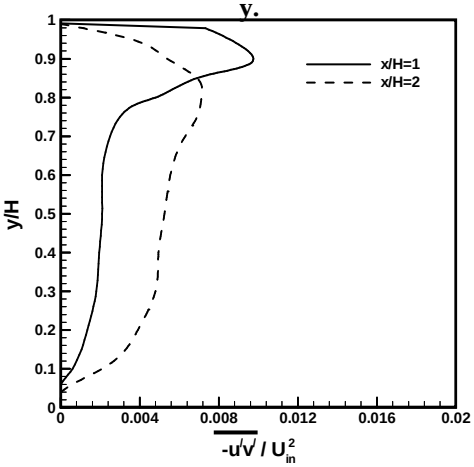

Figure (9) Distribution of Reynolds stress at horizontal cross section for Different location of y.

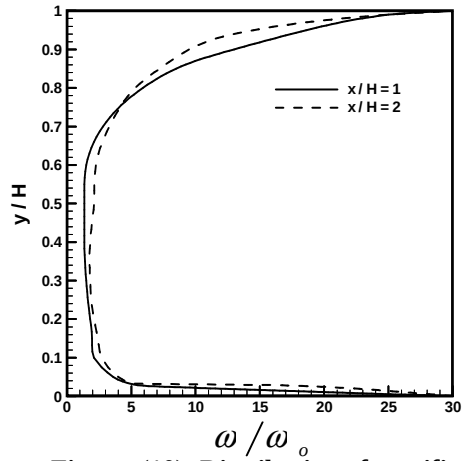

Figure. (10): Distribution of specific dissipation rate (ω) profile at vertical cross section

.

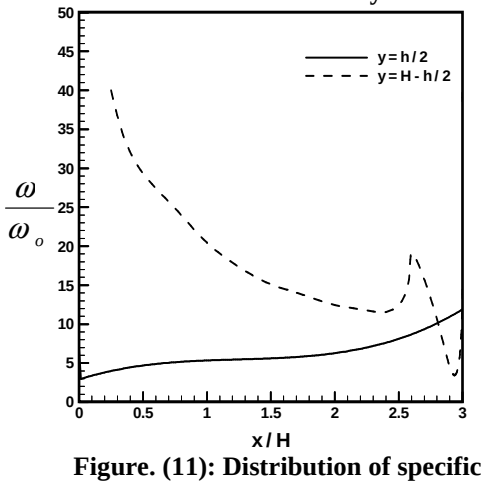

Figure. (11): Distribution of specific dissipation rate (ω) profile at horizontal cross section.

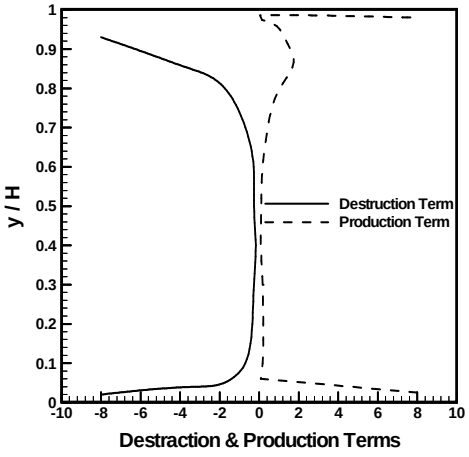

Figure (12): Distribution of destruction and production terms at vertical cross section for x=2H.

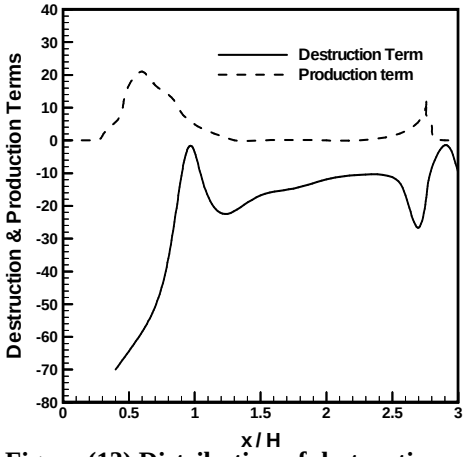

Figure (13) Distribution of destruction and production terms at horizontal cross section for y=H-h/2.

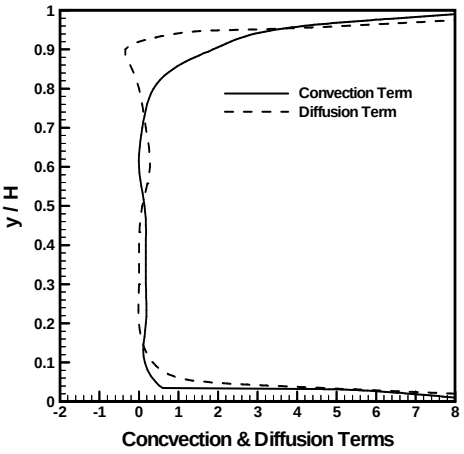

Figure. (14): Distribution of convection and diffusion terms at vertical cross section for x=2H.

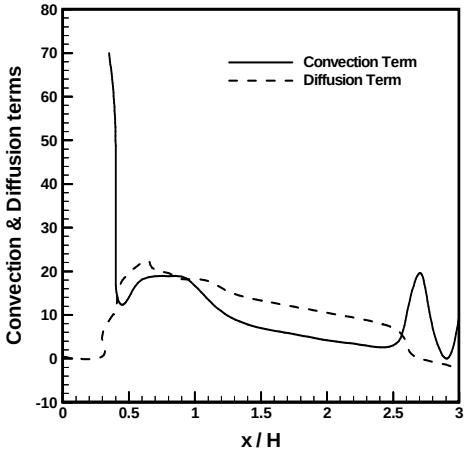

Figure (15): Distribution of convection and diffusion terms at horizontal cross section for y=H-h/2.

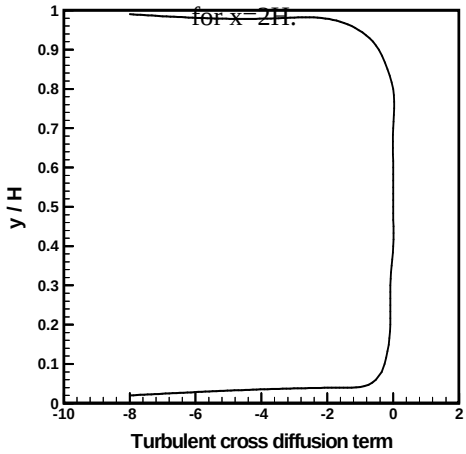

Figure. (16): Distribution of turbulent cross diffusion term at vertical cross section for x=2H.

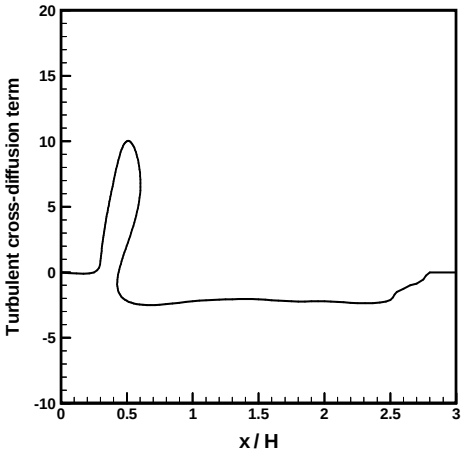

Figure. (17): Distribution of turbulent cross diffusion term at horizontal cross section for y=H-h/2.

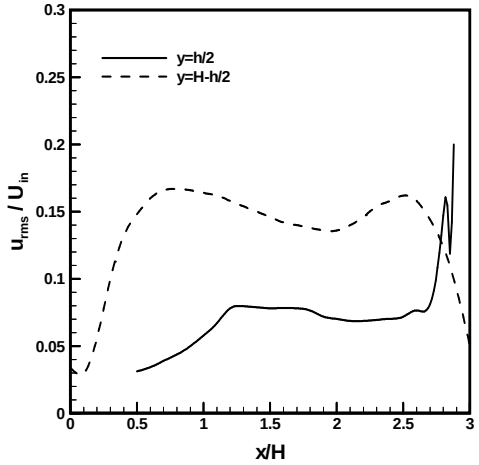

Figure. 18: Distribution of root mean square velocity fluctuation (u_{rms}) at y=H-h/2.

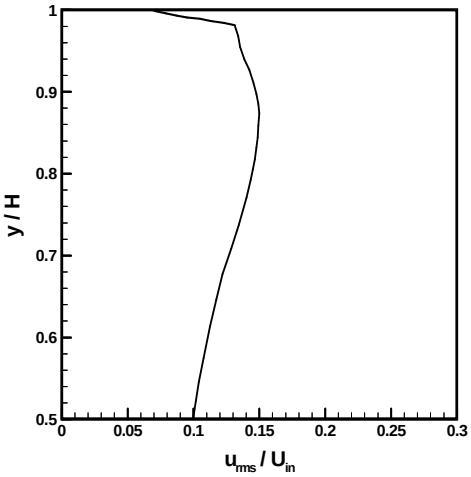

Figure. 19: Distribution of root mean square velocity fluctuation (u_{rms}) at x=2H.

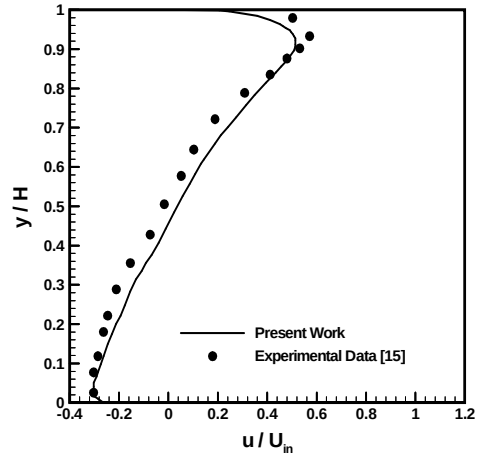

Figure. 20: Comparison between the present work and past work for Re=5000 at x/H=2.

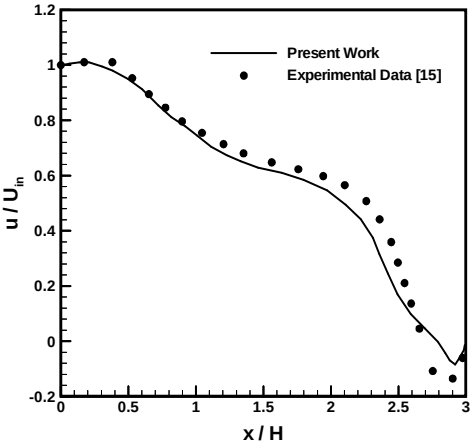

Figure. 21: Comparison between the present work and past work for Re=5000 at y=H-h/2.

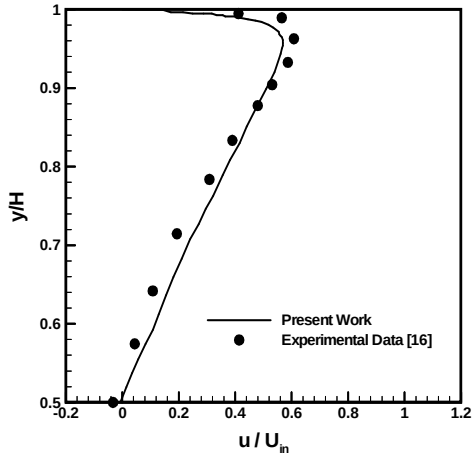

Figure. 22: Comparison between the present work and past work for Re=5000 at center line.

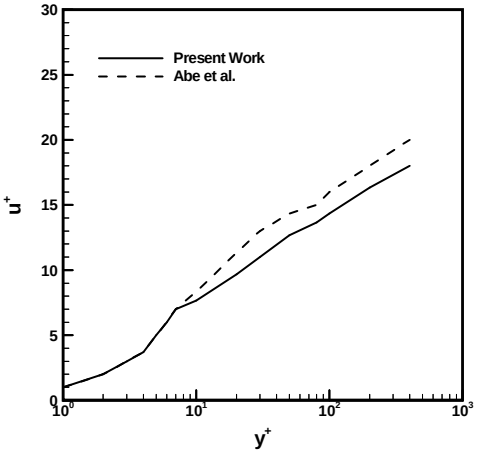

Figure. 23: Comparison between the present work and past work for channel flow at Re=10000.